High-Resolution Fluorine-19 Magnetic Resonance of Solids

ROBIN K. HARRIS

Department of Chemistry, University of Durham, South Road, Durham DH1 3LE, United Kingdom

PETER JACKSON*

ICI Specialties, Specialties Research Centre, P.O. Box 42, Hexagon House, Blackley, Manchester M9 3DA, United Kingdom

Received February 21, 1991 (Revised Manuscript Received July 3, 1991)

Contents

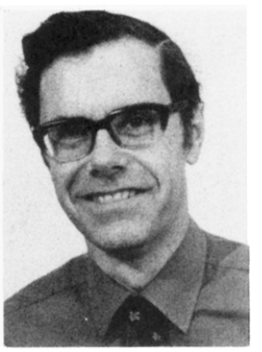

Robin Harris, born in 1936, was brought up in the London suburbs and studied for his B.A. and Ph.D. degrees at the University of Cambridge. The Ph.D. work, supervised by Norman Sheppard, was on NMR applications to chemistry. After two years post-doctoral experience at the Mellon Institute, Pittsburgh, he joined the staff of the "new" University of East Anglia in 1964, being promoted successively to a full Professorship in 1980. He moved to the University of Durham in 1984, where he is currently Chairman of the Chemistry Department. He has published over 250 research articles on NMR techniques and their chemical applications (lately concentrating on the solid state), including a textbook at graduate level. He is the Secretary-General of the International Society of Magnetic Resonance.

Peter Jackson was born in Stockport, England, in 1963. His B.Sc. was awarded by the University of East Anglia in 1984 and included one year spent at the University of Massachussetts at Amherst. He was awarded his Ph.D. in 1987 from the University of Durham after working on multiple-pulse solid-state NMR with Robin K. Harris. After spending one year with J. A. S. Smith working on relaxation and field-cycling NMR, he joined ICI plc as a specialist in NMR working in the Wilton Materials Research Centre. He is currently working in the ICI Specialties Research Centre, Manchester. His research interests include solid-state NMR (high-resolution and relaxation), hardware and techniques development and the use of NMR imaging in polymer and materials science applications.

I. Introduction

As illustrated by the various articles in this edition, NMR has assumed a primary role in the analysis of liquid-, solid-, and gas-phase samples in chemical, physical, biological, and materials laboratories. Where solid samples containing abundant nuclear spins (protons, ^1H, and fluorine, ^{19}F) are concerned, however, solid-state NMR experiments often fail to yield useful information, since they give rise to broad, featureless spectra. This is usually due to two predominant effects: (a) direct dipolar coupling (both homo- and heteronuclear) and (b) shielding anisotropy. Both can lead to significant line broadening which obscures spectral fine structure of interest, such as that arising from chemical shifts and scalar (indirect, J) couplings.

In liquids or solutions, rapid molecular tumbling averages both types of interactions to their isotropic values (zero for the dipolar interaction, isotropic chemical shifts in the case of shielding), yielding traditional high-resolution spectra, with line widths often below 1 Hz. Such spectra have proved to be invaluble for the determination of molecular structures. Solution-state ^{19}F NMR is characterized by a large chemical shift range (over 1000 ppm) and complex scalar coupling patterns. Chemical shifts have been observed, for example,[1] from −448 ppm (relative to $CFCl_3$) for ClF to +865 ppm for FOOF. For organofluorine derivatives,

* Author to whom correspondence should be addressed.

0009-2665/91/0791-1427$09.50/0

chemical shifts are more usually observed in the 0 to −200 ppm range. In solids, shielding anisotropies can be correspondingly large, meaning that, if dipolar coupling could be neglected, severely overlapping lines would still be observed from polycrystalline or unoriented static samples with more than one type of fluorine present. Such shielding anisotropies are inhomogeneous in character and can therefore be averaged by the now-standard solid-state method, magic-angle spinning (MAS),[2-4] yielding isotropic resonances and their associated sidebands at integral multiples of the spinning frequency.

Unfortunately, dipolar interactions normally cannot be neglected, with homonuclear dipolar interactions between fluorines in typical rigid solid materials, such as calcium fluoride, giving rise to spectral line widths in excess of 30 kHz (160 ppm for static samples at 4.7 T). If such interactions are homogeneous, i.e. dipolar coupling is strong and unmodulated by molecular motions, more-demanding experimental conditions are required to effect spectral narrowing. The spinning rates required for efficient averaging by MAS alone are in excess of the static dipolar interactions present. This means spinning at rates in excess of 10 kHz in many cases. The technology required to do this has only recently been introduced, but is now commercially available. However, as spinning speeds are increased, line widths are only reduced proportionally to the inverse spinning rate,[5] so that optimum line narrowing may require spinning speeds in excess of five times the relevant dipolar interactions. In the case of ^{19}F NMR, speeds in excess of 30 kHz may be necessary, given that the dipolar interaction between fluorines in a CF_2 group is ca. 7 kHz. Such rapid spinning speeds are not yet routine. On the other hand, if nuclei are relatively isolated, or are in special geometries (e.g. linear chains), or if anisotropic molecular motions are present, homonuclear dipolar interactions may be rendered inhomogeneous, allowing the use of more straightforward, moderate spinning rates (typically below 5 kHz). Where heteronuclear dipolar couplings are concerned, as between fluorines and protons, the situation is complicated further by homonuclear dipolar coupling between the protons: inhomogeneous heteronuclear interactions may be dominated by the proton–proton coupling, meaning that MAS rates in excess of the *proton–proton* dipolar interactions are required.

Several multiple-pulse sequences have been proposed as alternative methods for achieving homonuclear dipolar decoupling. These high-power, phase-alternated sequences, such as WAHUHA-4,[6] MREV-8,[7,8] and BR-24[9] all have the same basic ideal: suppression of the dipolar interaction while leaving behind shielding anisotropy information (albeit scaled by a sequence-dependent factor). Much of the pioneering work on such multiple-pulse sequences involved the observation of ^{19}F signals. The initial work of Waugh, Huber, and Haeberlen[6] concerned obtaining multiple-pulse spectra from a single crystal of calcium fluoride. The cubic symmetry around the F^- ion in the solid means that no shielding anisotropy is observed, offering a good test of dipolar decoupling efficiency. It is interesting to note that calcium fluoride was the early standard for comparisons of resolution, and has since been used as an internal reference standard, as well as being the subject of more recent high-resolution investigations itself. Such early multiple-pulse work[10,11] led to shielding tensors being measured in both powdered and single-crystal samples, adding greatly to the development of understanding of solid-state NMR parameters.

As indicated above, problems arise in multiple-pulse studies when more than one fluorine type is present in anisotropic environments for a given sample, resulting in overlapping resonances, from which the untangling of individual shielding tensor components is difficult if not impossible. This situation can be overcome in ^1H and ^{19}F solid-state NMR by combining the efficient dipolar decoupling performance of multiple-pulse sequences with MAS, giving isotropic chemical shifts at low spinning rates. The combined rotation and multiple-pulse spectroscopy (CRAMPS)[12] method was first illustrated with use of ^{19}F signals,[13] this time from a polymer sample, Kel-F. For CRAMPS operation to be effective, the important relationship is that between the multiple-pulse cycle time, t_c, and the MAS rotation period, t_r.[12] In order for the multiple-pulse sequence to decouple efficiently, the sample must "appear" to be stationary during one pulse cycle, i.e. $t_c \ll t_r$. In practice, this means spinning at rates below 5 kHz while using pulse cycles shorter than 100 μs. Thus even where homonuclear dipolar couplings and shielding anisotropies are large, high-resolution isotropic spectra may be generated by using only moderate spinning rates, with the possibility of shielding tensor information being retained in spinning sideband intensities.[14]

The theoretical background of the MAS, multiple-pulse, and CRAMPS experiments has been dealt with in great detail, so we will not consider these aspects further here. Rather, we concentrate on some of the practical aspects of rapid MAS and CRAMPS experiments and on illustrating the potential application areas for solid-state ^{19}F NMR by reference to existing work and other, as yet unreported, work from our laboratories. It is hoped that this will enable the reader to more fully appreciate the capabilities of these high-resolution methods and will therefore stimulate further work in as-yet unexplored fields.

Table I lists chemical shifts obtained by high-resolution solid-state ^{19}F NMR.

II. Magic-Angle Spinning

The introduction of MAS has been instrumental in establishing a whole range of analytical methods common in modern solid-state NMR laboratories. In particular, when combined with cross-polarization[15] (CP) and high-power proton decoupling,[16] high-quality, high-resolution spectra can now be obtained routinely from samples containing "dilute" spin 1/2 nuclei such as ^{13}C, ^{15}N, and ^{31}P. Sample-spinning techniques, including variable-angle,[17] dynamic-angle,[18] and double-axis rotation[19] methods, are now further extending solid-state NMR into studies involving quadrupolar nuclei, such as ^{17}O, ^{23}Na, and ^{27}Al.

A. MAS Experiments

The rise in popularity of MAS-based techniques has also led to improvements in sample spinning hardware. The early Andrew–Beams[20] rotor design ("mushroom rotor") was generally limited to spinning at rates below

TABLE I. Chemical Shifts Obtained by High-Resolution Solid-State ^{19}F NMR[a]

ref	sample	chemical group	chemical shift, ppm
33	LiF	F^-	−130
39	NaF	F^-	−221.0
33	NaF	F^-	−126
39	KF	F^-	−130.2
33	KF	F^-	−123
33	KF–CaF_2	F^-	−121
35	KF–alumina	F^-	−115
		AlF_6^{3-}	−156
34	KF–silica	SiF_6^{2-}	−129
36	$KAlF_4$	AlF_4^-	−155
36	K_3AlF_6	AlF_6^{3-}	−155
36	K_2SiF_6	SiF_6^{2-}	−92
33	RbF	F^-	−90
33	RbF·H_2O	F^-	−113
35	RbF–alumina	F^-	−109
		AlF_6^{3-}	−139
33	CsF	F^-	−79
33	CsF–CaF_2	F^-	−79
33	CsF·$2H_2O$	F^-	−97
33	CsF–alumina	F^-	−116
35	CsF–alumina	F^-	−88
		AlF_6^{3-}	−111
36	Cs_2SiF_6	SiF_6^{2-}	−92
39	MgF_2	F^-	−194.8
39	CaF_2	F^-	−104.8
50	CaF_2	F^-	−107.7
54	CaF_2	F^-	−106.4,−107.0
39	SrF_2	F^-	−84.1
39	CdF_2	F^-	−192.1
39	Hg_2F_2	F^-	−95.8
39	HgF_2	F^-	−196.4
39	SnF_2	F^-	−110.4
39	SnF_4	F^-	−146.9
39	FAP	$Ca_5(PO_4)_3F$	−98.9
54	FAP	$Ca_5(PO_4)_3F$	−101.0
31	FAP	$Ca_5(PO_4)_3F$	−99.0
28	FAP	$Ca_5(PO_4)_3F$	−99
39	FHAP	$Ca_5(PO_4)_3F_x(OH)_{1-x}$	−99 to −103[b]
		F^- (NSA)	−119
34	NH_4F–silica	SiF_6^{2-}	−128
33	Et_4NF–alumina	F^-	−123
33	$Et_4NF·2H_2O$	F^-	−130
33	Et_4NF–cytosine	F^-	−148
33	Bu_4NF–alumina	F^-	−106
33	$Bu_4NF·3H_2O$	F^-	−109
33	Bu_4NF–4-cyanophenol	F^-	−144
33	Bu_4NF–uracil	F^-	−149
33	Bu_4NF–$HOCPh_3$	F^-	−147
32	tremolite	F^-	−171.7
32	fluorscandium pargasite	F^-	−169.6
24	$(CF_2CFCl)_n$	$CFCl$	−130.2
		CF_2	−106.2,−100.2
37	$CH_2CF_2/CF_3CFCF_2/CF_2CFCl$ co- and terpolymers	$—CH_2CF_2CF(CF_3)CF_2CH_2—$	−71.9,−72.1,−72.7,−72.9
		$—CF_2CF_2CF(CF_3)CH_2CF_2—$	−76.4,−76.6,−77.6,−77.7
		$—CH_2CF_2CH_2—$	−82.1
		$—CF_2CH_2CF_2CH_2CF_2—$	−91.4,−91.8,−90.8,−91.5,−89.7
		$—CFClCH_2CF_2CH_2CF_2—$	−90.9
		$—CF_2CH_2CF_2CF(CF_3)CF_2—$	−104.4,−104.7
		$—CF_2CH_2CF_2CF_2CFCl—$	−108.8,−109.1
		$—CF(CF_3)CH_2CF_2CF_2CF(CF_3)—$	−112.8
		$—CF_2CH_2CF_2CF_2CF(CF_3)—$	−111.3,−111.6
		$—CF_2CH_2CF_2CF_2CH_2—$	−115.2,−116.7,−116.4
		$—CH_2CF_2CF_2CH_2CH_2—$	−116.8,−116.4
		$—CH_2CF_2CF_2CF(CF_3)CH_2—$	−119.3,−119.6,−120.0,−120.2
		$—CH_2CF_2CF_2CFClCH_2—$	−119.9,−120.2
		$—(CF_2)_n—$	−123.2,−123.6,−123.7,−123.8
		$—CF_2CF_2CFClCH_2CF_2—$	−122.3
		$—CF_2CFClCH_2—$	−127.7,−129.8,−130.5
		$—CH_2CF_2CF_2CF_2CH_2—$	−127.3,−126.7
		$—CF_2CF(CF_3)CF_2CF_2CF(CF_3)—$	−128.4,−130.5,−131.3
		$—CH_2CF(CF_3)CF_2CF_2CF(CF_3)—$	−135.7
		$—CF_2CF_2CF(CF_3)CH_2CF_2—$	−184.9,−185.0,−185.4,−185.8
this paper	$(CF_2CF_2)_n$	$—CF_2CF_2CF_2—$	−123.2
this paper	$(—C(CF_3)=C(CF_3)—)_n$	$CF_3—$	−50.2
		$CF_3—$	−54.1
this paper	$C_{20}F_{42}$	$CF_3—$	−82.4
		$CF_3CF_2—$	−127.9
		$—CF_2CF_2CF_2—$	−123.7
49, 53	$C_8F_{17}SO_3Na$	$CF_3—$	−83.0
		$CF_3CF_2—$	−129.8
		$—CF_2CF_2CF_2—$	−124.7
		$—CF_2SO_3—$	−118.2
50	Perfluoro-naphthalene ($C_{10}F_8$)	F_1	−146.9
		F_2	−148.4
		F_3	−151.7
		F_4	−152.6
51	$C_6F_5NH_2$	$F_{2,6}$	−165.2
		$F_{3,5}$	−167.7
		F_4	−177.8
this paper	AgTFA	CF_3COO^-	−71.5
41	$CFCl_3$/PU foam	$CFCl_3$	−2.0
41	$CFCl_2CH_3$/PU foam	$CFCl_2CH_3$	−45.6
41	$CHCl_2CF_3$/PU foam	$CHCl_2CF_3$	−79.6
this paper	$C_6H_4F—CO—$polymer	*p*-F	−108.5

[a] Results are only included where assigned and referenced chemical shifts have been reported. All shifts have been converted to the standard ^{19}F scale with δ ($CFCl_3$) = 0.0 ppm by using the following conversion factors: δ (PTFE) = −123.2 ppm; δ (C_6F_6) = −163.0 ppm. [b] Dependent on the value of *x*.

5 kHz, though higher speeds could be reached with smaller diameter designs and with helium, rather than air, as the spinning gas. Moreover, the angle setting was extremely sensitive to the rotor speed and sample density. While various laboratories have their own favorite design,[21-23] most commercial MAS probe manufacturers are currently using bullet-style rotors, driven by air forced onto a fluted cap and stabilized by gas bearings separate from the drive gas. This style of rotor is less sensitive to angle variations, and requires less regular calibration of the magic angle. Because of the rotor dimensions (7-mm diameter typical) and materials commonly used, spinning rates are, however, still limited to below 7 kHz in many commercial CP/MAS probes.

By scaling down the rotor dimensions and using an advanced polymer as the rotor material, it has been demonstrated[24] that spinning rates of up to 23 kHz can be achieved, with use of a helium/air mixture (at 26 psi) as the drive gas and air as the bearing gas. Commercial manufacturers are now producing fast spinning probes with performance to rival that above, although more routine (and less destructive!) rates of 10–17 kHz are often recommended. Results using spinning at 30 kHz have been more recently obtained.[25] These advances in spinning technology have enabled workers to study abundant, rather than dilute, spin 1/2 nuclei, using simple single-pulse/acquire sequences, with the increases in spinning rates allowing progressively more difficult materials to be studied. In the following sections, we use the terms slow spinning and fast spinning to denote work using rotation below and above the (arbitrary) rate of 7 kHz.

B. Slow-Spinning Applications

1. Mobile Polymers

Zumbulyadis and co-workers[26,27] have used ^{19}F MAS NMR with spinning at rates less than 4 kHz to study materials with either mobile polymer backbones or pendant, flexible side chains. In these situations, the anisotropic motions present are sufficient to partially average both dipolar interactions and shielding anisotropy. For example, in the case[27] of a fluoropolymer containing long chains of $-CF_2-O-CF_2-O-CF_2CF_2-O-$, two lines, approximately 2-kHz wide, are resolved in the *static* spectrum, as reproduced in Figure 1. By spinning the sample at the magic angle, the lines are narrowed further, leading to two groups of resonances with detailed fine structure, enabling polymer sequencing information to be deduced. It is even possible to observe polymer end-group effects, which give rise to other minor resonances, for example around −87 and −130 ppm. In such cases, where MAS can effectively suppress residual dipolar interactions, it has been shown that solid-state analogues of liquid-state two-dimensional experiments are possible. Thus a sample of a fluorinated polyphosphazene,[26] containing the side chains $-O-CH_2-CF_2-CF_2-CF_2-CF_3$, was used for a 2D solid-state NOESY experiment to give the unambiguous assignment of the side-chain resonances. With spinning at only 3.82 kHz, dipolar coupling (spin diffusion) is effectively quenched. The 2D cross-peaks observed can then be used to establish the fluorocarbon chain sequence. Even in such cases involving mobile species, residual line widths are still sufficiently large (of the order of 100 Hz) to obscure further fine structure due to fluorine–fluorine J couplings.

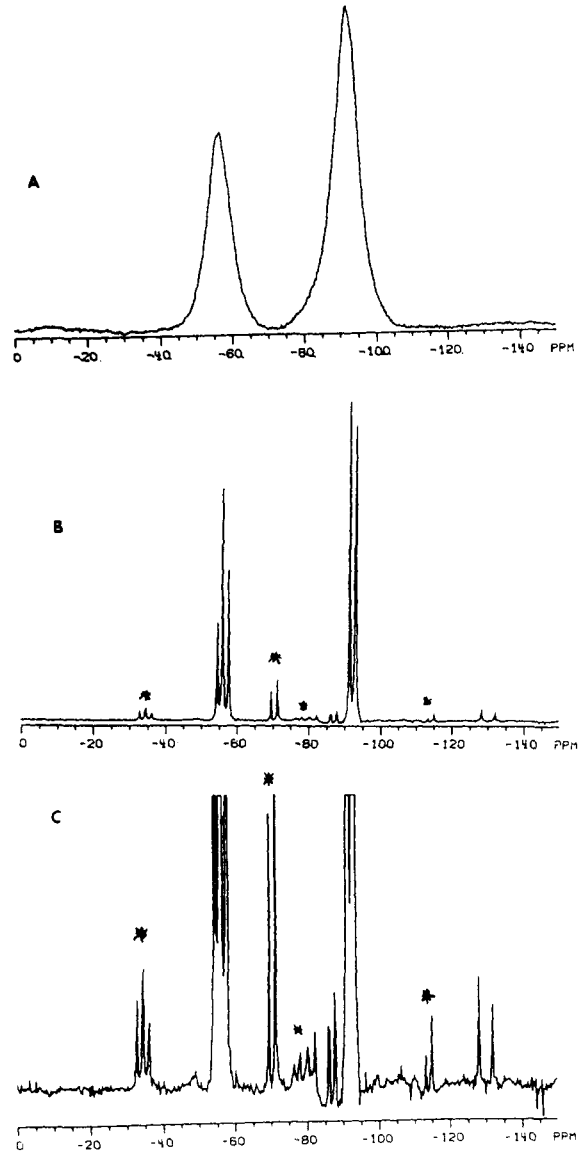

Figure 1. ^{19}F NMR (188.2 MHz) spectra of a fluoropolymer sample containing $CF_2-O-CF_2-O-CF_2CF_2-O$ chains: (a) static sample, (b) MAS spectrum, and (c) an expanded version of b. Spinning sidebands are marked with an asterisk (*). Polymer sequencing information may be deduced from the fine structure observed. Chemical shifts are referenced relative to external $CFCl_3$ (0.0 ppm). Figure reproduced courtesy of Dr. N. Zumbulyadis (Eastman Kodak).

2. Inorganic Fluorides

Yesinowski and co-workers[28-30] have pioneered the use of ^{19}F MAS NMR in the study of the fluoridation of dentally important apatites. For fluoroapatite (FAP), $Ca_5(PO_4)_3F$, and fluorohydroxyapatite (FHAP), $Ca_5(PO_4)_3(OH)_{1-x}F_x$, the fluorine-19 signals are inhomogeneously broadened, allowing relatively slow MAS (3–4 kHz) to be used to obtain high-resolution spectra (see section II.C.3). In addition, under these conditions, homogeneously broadened signals from calcium fluoride are not narrowed, allowing the differentiation of the fluoride types present.

The spectrum observed[28] from a sample of hydroxyapatite (HAP) several days after exposure to 9.7 mM

F^- solutions indicated the formation of a surface layer of FHAP, with $x = 0.4$ to 0.8 in the above formula. The same sample studied six months later gave a spectrum identical with that of bulk FAP, and, subsequently, no further aging was observed. The authors indicated that this solid-state transformation was probably due to ion migration over the surface, rather than a bulk phase transformation. Exposure of HAP to solutions with higher levels of F^- gives rise to samples containing significant levels of calcium fluoride. The lack of line narrowing of the calcium fluoride resonance made quantitative measurements difficult. The development of rapid spinning hardware has led to improved quantitative measurements in such systems, as described later.

Doped FAP materials (phosphors) are commonly used in fluorescent lights, since such materials can emit light on UV irradiation. MAS has been used[31] to identify and quantify the presence and site of antimony (Sb^{3+}) activators in a range of substituted FAP samples, with the ^{19}F spectra showing shifted peaks and shoulders attributable to substitution and correlating with increasing antimony content. This work also indicated that crystallite sizes or crystal defects are important in determining FAP line widths, since the phosphor samples give rise to unperturbed FAP signals 5-fold narrower than those previously obtained from other FAP samples.

Raudsepp et al.[32] have used ^{19}F NMR with MAS at 3.5 kHz to look at differences in fluorine sites in the synthetic minerals tremolite and fluorscandium pargasite. Fluorine in the latter material gives rise to a signal with a more extensive spinning sideband pattern, indicating a greater local asymmetry. The spectrum also exhibited a broadened centerband, as well as shoulders on the sidebands, indicating the presence of two fluorine sites, with coordination to MgMgMg and MgMgSc.

Using spinning at ca. 3 kHz, Clark et al.[33] have probed chemical shifts in some ionic fluorides in order to improve on similar studies performed in solution. In the solid state, a much wider range of F^- environments exists than in solution, giving rise to an increased chemical shift range. Samples of LiF, NaF, KF, RbF, CsF, Et_4NF, and Bu_4NF were studied as the pure salts as well as in hydrates (where formed). Some samples were also deposited onto calcium fluoride and alumina surfaces, as a precursor to further work on catalysis. On alumina, strong hydrogen bonding to surface hydroxyl protons gave large chemical shift changes. Some anhydrous quaternary ammonium complexes were also prepared to study the effects of F···H hydrogen bonding. Chemical shifts observed ranged from −79 ppm for anhydrous CsF to −149 ppm for a Bu_4NF·uracil complex with a strong N–H···F hydrogen bond. The chemical shifts observed are collected, together with the others reported in this article, in Table I. Under the slow spinning conditions used, no narrowing of the spectrum of the calcium fluoride support was observed.

3. Catalysis

The above work has been extended to study the adsorption of fluoride-containing species onto silica,[34] alumina,[35] and montmorillonite clay.[36] By adsorbing MF species (M = NH_4, Na, K, Rb, Cs) onto montmorillonite K10 at various loadings (0.5, 2, 3.5, 5, and 10 mmol MF/g K10) and drying the resulting samples at a range of temperatures, a variety of complex fluorides was formed. Resonances in some of the MAS spectra could be readily assigned to known species, such as SiF_6^{2-}, AlF_4^-, and AlF_6^{3-}, in agreement with concurrent FTIR analyses. Peaks due to other expected species, such as chemisorbed, surface Si–F, could not be unambiguously identified in the NMR spectra due to residual line broadening and extensive spectral peak overlap, obtained because of the substantial spinning sideband patterns produced from such asymmetric fluorine species.

Fluorination of silica gel with KF, Na_2SiF_6, NH_4F, and $(NH_4)_2SiF_6$ has been studied,[34] with ^{19}F MAS NMR results illustrating to good effect the difference between samples prepared with ammonium- and sodium-containing reagents. With KF–silica, a resonance due to SiF_6^{2-} is readily identified, the presence of which accounts for the poor reactivity of this modified silica material. On the other hand, NH_4–silica has enhanced catalytic properties. The NMR results point to this being due to the presence of chemisorbed HF, present as surface Si–F species. In this case, the relatively slow spinning rate (leading to large residual line widths), and the large shielding anisotropy, again did not allow unambiguous determination of the isotropic chemical shifts. Similar work on MF–alumina[35] (where M = Na, K, Rb, Cs), in conjunction with IR spectroscopy, shows that in each case studied, AlF_6^{3-} species are formed, with MAS NMR allowing the identification of separate MF and AlF_6^{3-} resonances. NMR could not differentiate between AlF_4^- and AlF_6^{3-} in model compounds since both species give rise to signals at −155 ppm with large line widths. Such line broadening could be due to residual dipolar coupling or quadrupolar-modified heteronuclear dipolar interactions with the aluminum (spin 5/2, quadrupolar nucleus).

C. Fast-Spinning Applications

1. Fluoropolymers

The benefits of rapidly spinning more difficult materials were originally illustrated[24] by reference to, among examples with other nuclei, ^{19}F spectra of a sample of the rigid polymer poly(chlorotrifluoroethene), $-(CF_2CFCl)_n-$, trade name Kel-F (3M Corporation). By spinning at 16.8 kHz, three separate resonances could be clearly identified at 23, 17 (CF_2), and −7 (CFCl) ppm (relative to PTFE), with spectral narrowing only becoming effective when spinning at rates above 8.5 kHz (Figure 2). The reason for the observation of two assigned CF_2 resonances was not clear, but was considered to be consistent with a simple, highly ordered isotactic structure.

More detailed work has since been published[37] on a variety of co- and terpolymers containing vinylidene fluoride, VDF (CF_2CH_2) in conjunction with: (a) hexafluoropropene, HFP (CF_2CFCF_3), (b) HFP and tetrafluoroethene, TFE (CF_2CF_2), and (c) chlorotrifluoroethene, CTFE (CF_2CFCl). The high density of fluorine in these polymers means that spectral lines are homogeneously broadened, requiring spinning at rates between 18.0 and 20.1 kHz to obtain chemically resolved peaks. The high resolution obtained at such

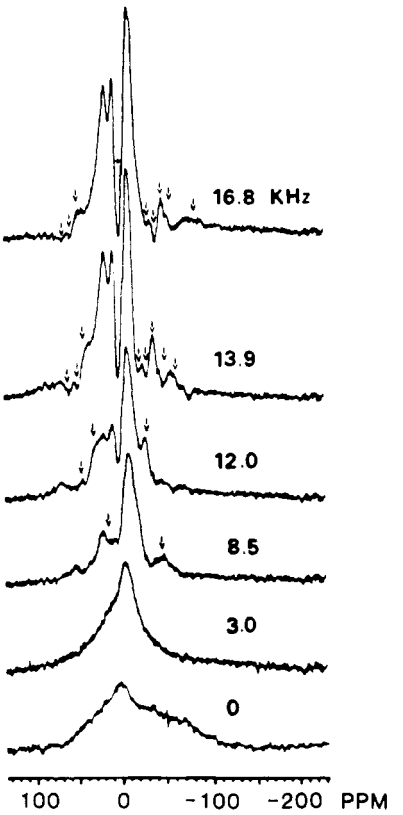

Figure 2. ^{19}F MAS NMR (338.7 MHz) spectra of a Kel-F polymer as a function of spinning speed. The arrows indicate spinning sidebands. The chemical shift scale is referenced to PTFE (0.0 ppm) (reprinted from ref 24, copyright 1986 Academic Press).

spinning rates allows the deduction of polymer microstructure out to five-carbon chain sequences (pentads). The presence of different structural moieties gives rise to peaks ranging from 50.3 ppm (relative to PTFE) for the CF_3 resonance in the $-CH_2-CF_2-CFCF_3-CF_2-CH_2-$ carbon pentad to −62.2 ppm for the CF resonance in the $-CF_2-CF_2-CFCF_3-CH_2-CF_2-$ pentad. Although rapid spinning was performed, some spectral overlap is observed, but by curve fitting it is, for example, possible to identify up to 11 components in the spectrum of a VDF/HFP copolymer, as illustrated in Figure 3. The quantitative measurement of such sequencing information obtained by ^{19}F fast MAS NMR not only allows detailed pictures of polymer structure to be formed, but also helps to measure important polymerization reaction rate parameters if, for example, original monomer feed-stock ratios are known.

More complex polymeric species, produced by plasma polymerization, have also been studied by using fast-spinning ^{19}F NMR.[38] Such materials are of increasing importance in industry as coatings and surface modifiers. Figure 4 shows the spectrum from a typical material produced from a hexafluoropropene (HFP) plasma. Under these vigorous conditions, a variety of reactive radical and charged species are formed, giving rise to a highly irregular, highly crosslinked polymer containing many defects and trapped radicals, which means that spectral lines are exceedingly broad, even with fast spinning, due to chemical shift dispersion and possible interactions with unpaired electrons. Nevertheless, at least seven individual lines may be distinguished from the broad background signal, three of which are in the characteristic CF_3 region of the spectrum, at −61, −73, and −83 ppm. By comparison with reference chemical shifts,[1] these may be tentatively assigned to the following possible structures: −83 ppm, $CF_3—CF_2—$; −73 ppm, $CF_3—C<$, $CF_3—CF=C<$; −61 ppm, $(CF_3)_3C—$, $(CF_3)_2C<$, $(CF_3)_2C=C<$ It is more difficult to assign the other resolved peaks in the

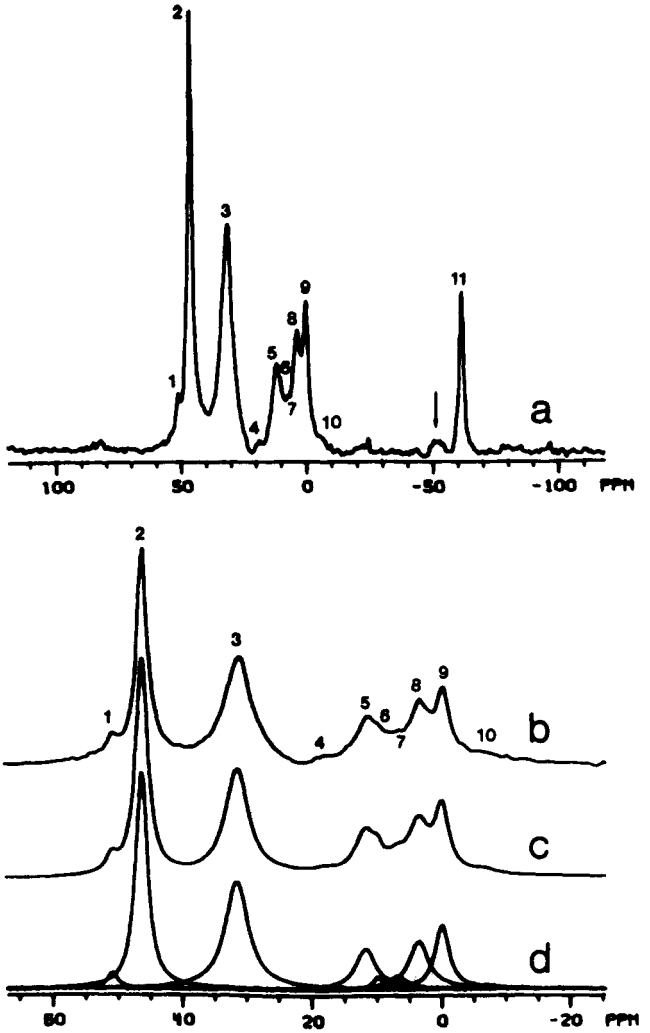

Figure 3. ^{19}F MAS NMR (338.7 MHz) spectra of a VDF/HFP copolymer: (a) spinning at 18.0 kHz (the arrow indicates a spinning sideband), (b) expansion of the CF_3 and CF_2 region of the spectrum, (c) computer simulation, and (d) deconvoluted peaks derived from c. The chemical shift scale is referenced to PTFE (0.0 ppm) (reprinted from ref 37, copyright 1987 American Chemical Society).

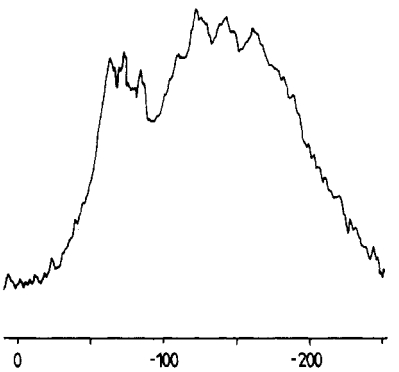

Figure 4. ^{19}F MAS NMR (188.3 MHz) spectra obtained from a polymeric material formed by plasma deposition of HFP. Chemical shifts are referenced relative to external $CFCl_3$ (0.0 ppm). The spinning rate used was 12.5 kHz.

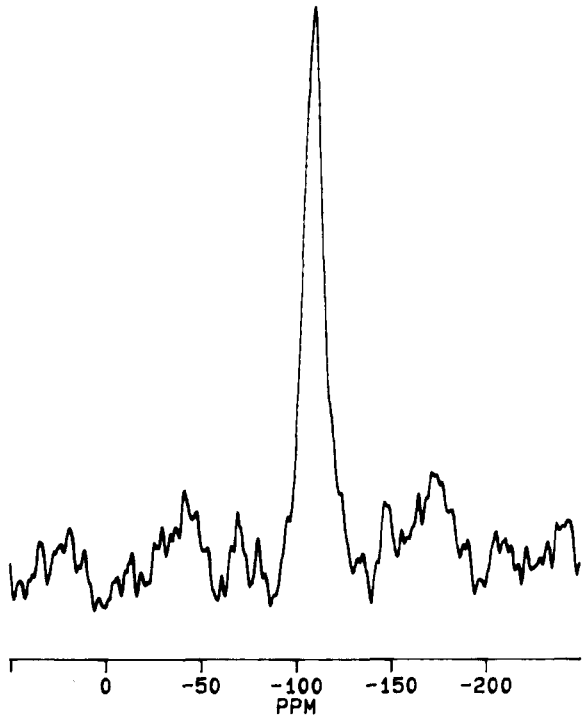

Figure 5. ^{19}F MAS NMR (188.3 MHz) spectrum of an experimental nonfluorinated aromatic polymer containing fluorinated end groups, obtained with spinning at 10.0 kHz. The chemical shift is characteristic of a fluorine on a benzene ring in the para position to a ketone linkage. Chemical shifts are referenced relative to external $CFCl_3$ (0.0 ppm).

spectrum to specific structures, since a wide variety of CF_2 and CF environments are possible, also contributing to the broad background. Such results may be used to correlate processing conditions with chemical structure and help to optimize experiments to produce the desired final properties.

2. Other Polymer Applications

It has been possible to use fast MAS to quantify the end groups present in model and industrially important high-performance aromatic polymers. One method of preparation of some systems involves the polymerization of monomer units having the following general reactive ends: F–Ar–R and HO–Ar–R′, generating R–Ar–O–Ar–R′ linkages, and eliminating fluorine from the polymer chain. Reactions may be prematurely terminated by addition of nonfluorinated end groups, allowing the measurement of end-capping efficiency by quantitative observation of the ^{19}F fast MAS NMR signals. Figure 5 shows a typical spectrum from a sample containing less than 0.03 mol % fluorine, which is indicative of fluorine in a phenyl chain end, in the para position to a ketone linkage. In such polymer systems, even though the fluorines are extremely dilute, fast MAS is still required to obtain high-resolution spectra. This is due to strong heteronuclear dipolar coupling to the surrounding protons which are themselves strongly homonuclear dipolar coupled. Because of the low concentration of fluorine present, it is extremely difficult to obtain reliable wide-line, dipolar-broadened spectra from these systems (especially where probeheads have small levels of fluorine background signals), but the line-narrowing effect of fast MAS allows useful spectra to be obtained in less than 30 minutes.

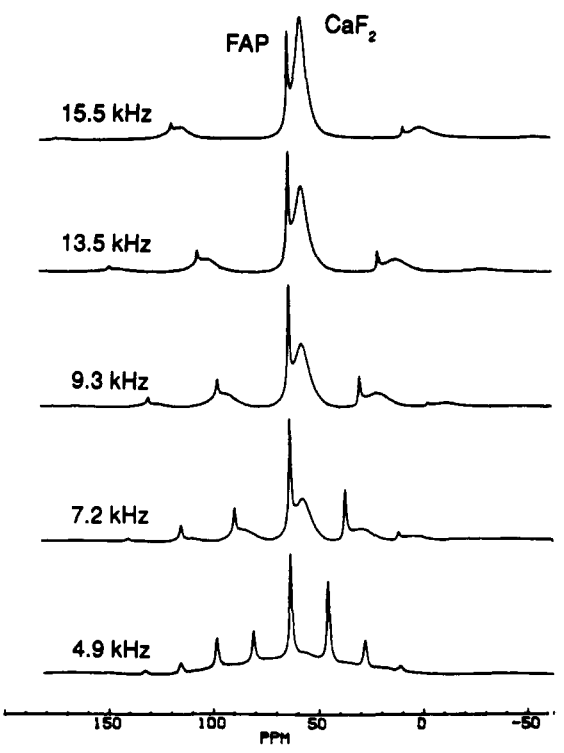

Figure 6. ^{19}F MAS NMR (282 MHz) spectra of an 80:20 mixture of CaF_2 and FAP as a function of spinning speed. The FAP resonance is narrowed at even the lowest spinning speeds, whereas the strong dipolar coupling present in CaF_2 means that rapid spinning is required to effect narrowing. The CaF_2 line width has not reached a minimum value at 15.5 kHz. Chemical shifts are referenced relative to external C_6F_6 (0.0 ppm) (reprinted from ref 39, copyright 1990 Academic Press).

3. Inorganic Fluorides

The potential of fast-spinning techniques to further extend studies of fluorinated apatites and metal fluorides has been identified by Kreinbrink et al.[39] By using spinning rates up to 15.5 kHz, it has been possible to improve the quantitation of FAP/CaF_2 mixtures by obtaining spectra with lines from both phases narrowed. This is in contrast to the earlier work described in section II.B.2, which used slow spinning, where the CaF_2 resonance was broad, essentially unaltered from the static spectrum. Figure 6 shows the improvement in resolution and quality obtained as the spinning rate is raised from 4.9 to 15.5 kHz. At the highest spinning rate, with use of spectral simulation and deconvolution, it is possible to quantify mixture compositions in the 5–50 wt % CaF_2 range to better than 95% accuracy. To aid further investigations into dental processes, a range of metal fluorides was also studied. Such materials are present in either biological apatites or in commercial dentifrices. This work also extends the earlier studies on inorganic fluorides to include those (such as calcium fluoride) that give no line narrowing at slower MAS rates. Figure 7 nicely illustrates the range of chemical shifts observed, from 78.9 ppm (relative to C_6F_6) for SrF_2 to −58.0 for NaF (although the difference of 95 ppm between this result for NaF and that found by earlier workers[33] indicates that some further work may be required on this particular salt). In addition to the differences in chemical shift, residual line widths (spinning at 12.5 to 15.5 kHz) ranging between 430 Hz for SnF_2 and 4.83 kHz for SnF_4 were observed for the metal salts. The authors also pointed out that improved

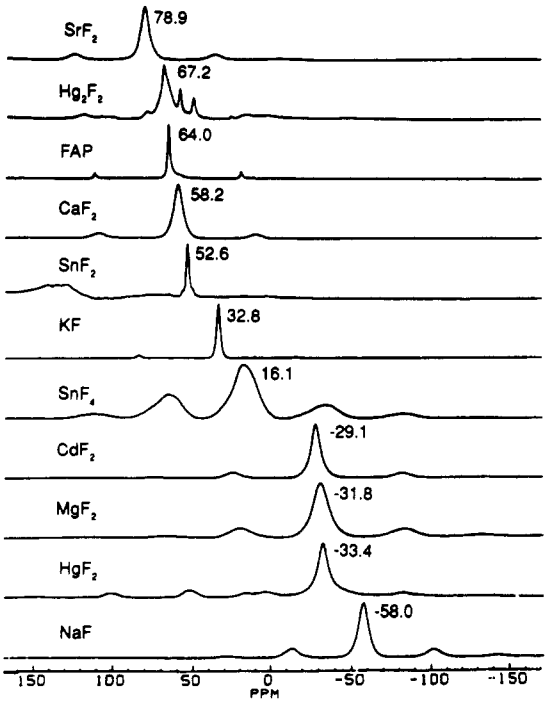

Figure 7. ^{19}F MAS NMR (282 MHz) spectra of several inorganic fluoride species, obtained with spinning speeds between 12.5 and 15.5 kHz. The chemical shift scale is referenced relative to external C_6F_6 (0.0 ppm) (reprinted from ref 39, copyright 1990 Academic Press).

resolution would be expected at even higher spinning rates, since lines were continuing to narrow as spinning rates were increased, even at 15.5 kHz.

The resolution gained by fast spinning allowed the more-detailed investigation of the reaction of F^- with apatitic surfaces. After titrating HAP with aqueous NaF (50 ppm F^-) at physiological pH, it was possible to observe a peak at δ_F = 44 ppm (from C_6F_6) attributable to nonspecifically adsorbed (NSA) F^-. At higher concentration levels, specific adsorption of F^- occurs, leading to exchange of NSA fluoride for OH in surface sites, giving rise to a FHAP peak in the fast MAS spectrum. Further, more detailed work using the rapid spinning technique is promised in this area.

4. *Analysis of Polymer Foam Blowing Agents*

By using liquid-state ^{19}F NMR, it has been possible to identify gas-phase chlorofluorocarbon (CFC) blowing agents trapped in polyurethane (PU) foams.[40] In addition to the sharp gas-phase peaks, a broad signal was observed from CFC molecules absorbed into the solid polymer. Since the fluorines in such rigidly held molecules are strongly dipolar coupled, both to other fluorines, protons and chlorine in the same molecule (where present), and to protons in the polymer matrix, fast spinning gives the possibility of narrowed spectra, allowing the further identification of different CFC components in the "polymer phase". A sample of a commercial PU foam made with a model blowing agent formulation containing a 1:1:1 molar ratio of $CFCl_3$, $CFCl_2CH_3$, and $CHCl_2CF_3$ has been studied, with spinning at 11 kHz. The results are shown in Figure 8. Spinning at 2.1 kHz gives a spectrum showing only peaks arising from the gas-phase CFCs trapped in the cells of the foam sample. Spinning at 11 kHz is sufficient to allow signals from polymer phase CFCs to be

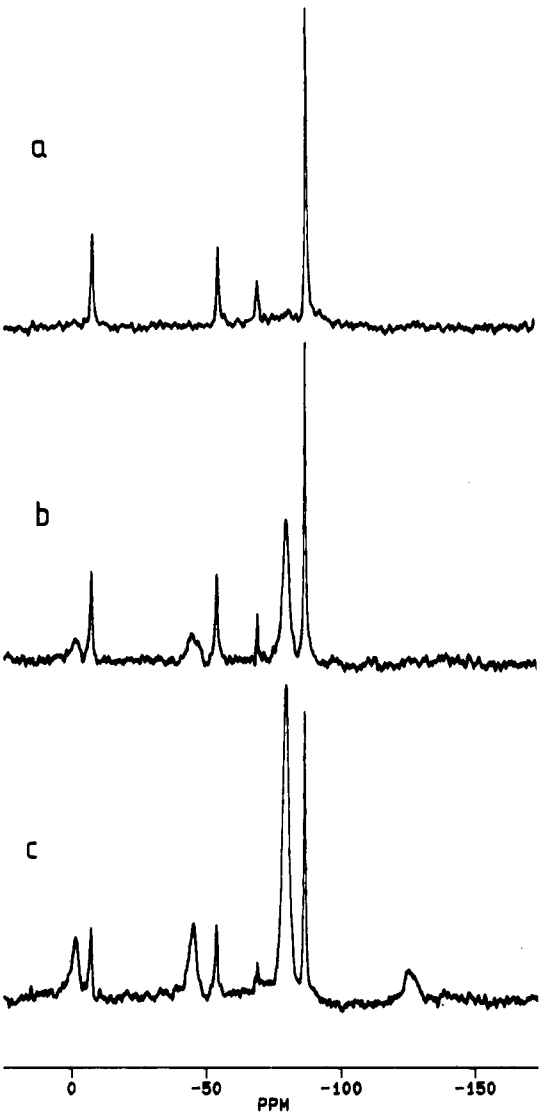

Figure 8. ^{19}F MAS NMR (188.3 MHz) spectra of polyurethane foam samples containing fluorinated blowing agents: (a) sample obtained from a foam block center with spinning at 2.1 kHz, (b) same sample as a, but spinning at 11.0 kHz (signals from both gas phase and polymer phase fluorines are now observed), and (c) sample taken from the foam block edge, with spinning at 11.0 kHz. A further as-yet-unidentified peak is apparent. Chemical shifts are referenced relative to external $CFCl_3$ (0.0 ppm).

unambiguously assigned, with chemical shift differences between polymer and gas-phase signals which may be attributable to differences in bulk susceptibility. By taking two samples, one from the edge and one from the center of a foam block, it was possible to show that degradation had occurred in the polymer phase at the block edge by the growth of an unidentified resonance at −125.4 ppm (from liquid $CFCl_3$).

D. Future Developments

Even though the introduction of rapid spinning probeheads has led to a dramatic improvement in the resolution possible from fluorinated samples, results have shown that even better resolution may be achieved by extending accessible spinning rates above 20 kHz. In many cases, line widths are still improving at the highest speeds possible on presently available fast MAS probes. Implementation of a commercial 30-kHz probehead is eagerly awaited by fast MAS practitioners!

Nevertheless, useful spectra can be acquired by using present technology, and it is expected that the range of problem types tackled will rapidly expand, especially in pharmaceutical and agrochemical areas. MAS will undoubtedly play a more leading role in the understanding of fluoridation processes in dental applications, and rapid spinning methods should allow more-detailed information to be obtained from catalytic materials. The use of ^{19}F MAS NMR in the study of the interaction between materials and CFCs will no doubt increase in importance as more environmentally acceptable (but less well chemically characterized) alternatives are introduced.

Since fast spinning suppresses dipolar interactions, it should be possible to monitor NMR relaxation parameters in the absence (or with a considerable reduction) of spin diffusion, especially useful in polymer science applications. By performing variable spin-locking experiments in conjunction with fast MAS it will be possible to correlate spectral features with particular morphological regions. It should also be possible to obtain quantitative information on relative domain proportions (e.g. percentage crystallinity) by measuring peak intensities as a function of spin-lock time (i.e. from individual T_1 measurements) by relaxation curve deconvolution, since spin diffusion is suppressed. Two-dimensional experiments, as exemplified by the slow-spinning application (NOESY) discussed earlier, should also become more straightforward in the absence of strong dipolar line broadening.

III. CRAMPS

In a recent article, Dec et al.[42] illustrated that, for rigid proton-containing samples, superior resolution was always obtained by use of ^1H CRAMPS rather than by fast MAS alone, even when spinning rates up to 21 kHz were used. Despite spinning at rates in excess of the expected dipolar interactions, residual line widths still contained contributions from incompletely averaged ^1H–^1H dipolar interactions, reflecting the general inverse relationship between centerband line width and spinning rate. This has also been noted experimentally in ^{31}P MAS NMR, although the spinning rates required for efficient dipolar decoupling are generally much lower (ca. 5 kHz). Even so, at intermediate spinning rates, in excess of the magnitude of the expected dipolar interactions, ^{31}P CRAMPS (with proton decoupling) gave rise to narrower lines than by spinning alone. It was also noted by Kreinbrink et al.[39] that the residual ^{19}F line widths obtained from samples of calcium fluoride and sodium fluoride decreased steadily as spinning was increased from 6 to 15 kHz, and had not reached a constant value. Thus it would seem that ^{19}F CRAMPS has the potential to achieve improved resolution over that already achieved by MAS alone, even at high spinning speeds.

A. CRAMPS Experiments

The multiple-pulse sequences most often used with CRAMPS are MREV-8[7,8] and BR-24.[9] To illustrate the important parameters associated with multiple-pulse operation, the MREV-8 sequence, shown in Figure 9, will be considered in more detail here. During multiple-pulse acquisition, the signal is sampled in a pointwise fashion during the long (2τ) window of the sequence. In order to do this, the probe circuitry must ring down rapidly following the preceding pulse. Otherwise, the NMR receiver will be saturated, obscuring the NMR signal of interest. This means that the minimum MREV-8 cycle time that can be used is 12τ or $6t_d + 6t_w + 6t_s$, where t_d is the ring-down time, t_w is the pulse width, and t_s is the data sampling time. The cycle time used is important on three counts: (a) it has been shown[44] that optimum resolution is obtained by using the shortest possible cycle times, (b) cycle times must be kept short to satisfy the CRAMPS condition that $t_c \ll t_r$, and (c) the signal digitization rate is fixed by the cycle time, leading to a limitation in accessible spectral widths. This is especially important for fluorine observation, where large chemical shift differences may be observed.

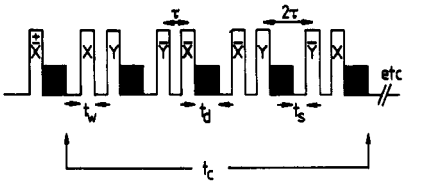

Figure 9. The MREV-8 multiple-pulse sequence. Quadrature rf pulse phases are denoted by ±X, ±Y. The cycle consists of 8 pulses, of duration t_w, with $\tau - 2\tau$ timing intervals and a total cycle time, t_c. Following the probe ringdown time, t_d, data points may be taken during the long (2τ) windows in a time, t_s. The total cycle time is then 12τ, or $6t_d + 6t_w + 6t_s$.

Most commercially available MAS probes are capable of performing CRAMPS experiments to some extent, since ring-down times are often less than 10 μs. However, for ^{19}F CRAMPS, two different approaches have been made to obtaining shorter cycle times: probe "Q-spoiling" and single-point acquisition. Spoiling the Q of the probehead has been achieved[45] simply by adding resistance to the rf circuit, with MREV-8 cycle times as short as 30 μs possible, together with 90° pulse lengths of 1.5 μs. Q-spoiling has the disadvantage of requiring higher power levels to obtain a given 90° pulse length. The single-point approach[46] uses the ideas first proposed[44] for low-power multiple-pulse decoupling, where windowless and semiwindowless sequences are used. The signal is built up in a pointwise fashion at the end of an incremented number of cycles, dispensing with the need for sampling during the pulse train. This allows the MREV-8 sequence to be shortened to the semiwindowless limit and has been shown to increase the available spectral width by a factor of 3 with use of a commercial probe. There is an obvious time penalty associated with this method, although this is somewhat offset by being able to get more signal back from higher-Q probes.

In addition to the cycle-time dependence of resolution, multiple-pulse sequences are also sensitive, to varying degrees, to offset. It is the authors' experience that a well-tuned MREV-8 sequence will perform as well as BR-24 close to resonance, but resolution is degraded further at larger offsets. Operating at shorter cycle times reduces the offset dependence, so there is an advantage in operating with the smallest possible offsets. For ^1H operation, this is always practicable, since there is only a relatively small chemical shift range (0–20 ppm, 4 kHz at 4.7 T) and spinning sidebands are rarely observed. As we have seen, with fluorine a chemical shift range of 0 to −300 ppm might be more

typical, accounting for chemical shifts and spinning sidebands, giving potential offsets of 60 kHz at 4.7 T. Despite CRAMPS signals being traditionally acquired in nonquadrature mode, quadrature information may be extracted from CRAMPS signals in two ways. It has long been recognized[47] that by combining the signals obtained from different 2τ windows in the MREV-8 sequence, and correctly scaling the results, quadrature spectra can be obtained. This requires post-processing, but also potentially improves data-sampling rates, allowing wider spectral widths. The other approach, used with the single-point acquisition method, is to correctly scale the data prior to acquisition by applying a 45° pulse, allowing the data obtained to be Fourier transformed directly using standard spectrometer software.

If CRAMPS experiments are to be successful, the multiple-phase component must be properly adjusted. There are now well-established routines[45,48] for tuning a spectrometer to ensure that pulse amplitudes and phases are optimized, and that other experimental parameters, such as transmitter power droop and phase transients ("glitch") are minimized. Standard samples for setting up the spectrometer for ^{19}F operation include the liquids C_6F_6 and $CFCl_3$, as well as the rubbery solid material poly[(trifluoromethyl)vinylmethylsiloxane].[46] Fine tuning of the offset frequency at a particular spinning rate may also be required to minimize "rotor line" artefacts in a spectrum.

B. CRAMPS Applications

Fluorine-19 CRAMPS NMR spectra have been shown to offer the potential for high-resolution, efficiently dipolar-decoupled spectra, with the added "bonus" of shielding anisotropy information retained in spinning sidebands. The results of CRAMPS investigations have been collected together, and spectral parameters are reported in Table I. Individual results are discussed in more detail in the following sections.

1. Fluoro-Organic Molecules

The application of the single-point acquisition method was demonstrated[46] by using a sample of silver trifluoroacetate, AgTFA. Figure 10 shows the benefit that may be gained from CRAMPS operation. Due to mobility of the CF_3 groups in the solid state, the dipolar broadening, which dominates the static spectrum, can be reduced by spinning at only moderate rates. At 6 kHz, spinning sidebands are formed, with intensities due to residual dipolar interactions and shielding anisotropy, and the centerband is narrowed to 1400 Hz. At 12.5 kHz, the AgTFA centerband line width is 860 Hz, and the spinning rate is faster than the magnitude of the shielding anisotropy, so the small remaining sidebands are now essentially only of dipolar origin. CRAMPS operation (single-point method), on the other hand, allows efficient removal of the dipolar broadening, resulting in narrow lines (less than 100 Hz, although exponential line broadening has been added to minimize truncation artefacts) and spinning sidebands due purely to shielding anisotropy, with spinning at only 2.0 kHz (although the multiple-pulse scaling factor gives an apparent spinning rate of ca. 4.0 kHz). The CRAMPS resolution obtained under the single-point method is better than that obtained by using conventional nonquadrature detection, where a line width of

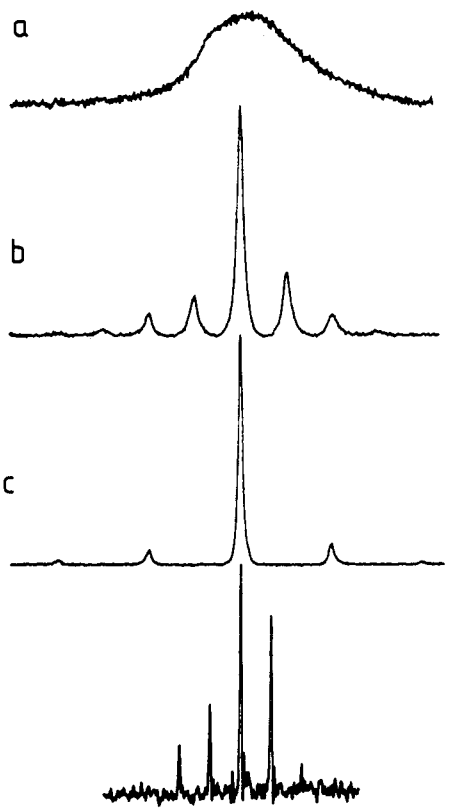

Figure 10. ^{19}F NMR (188.3 MHz) spectra of AgTFA: (a) single pulse spectrum, static sample, (b) MAS spectrum, spinning at 6.0 kHz, (c) MAS spectrum, spinning at 12.5 kHz, and (d) spectrum using single-point MREV-8 CRAMPS (t_c = 36 μs) with quadrature detection and spinning at 2.0 kHz.

440 Hz was observed.[49] This difference is no doubt due to the smaller offset frequency allowed by quadrature detection used with the single-point experiment. Analysis of the CRAMPS spinning sidebands would, of course, allow the calculation of the fluorine shielding tensor components.

In the case of AgTFA, the fluorine T_1 relaxation times are sufficiently short to allow single-point acquisition with a recycle delay of 3 s. For other, more rigid fluorinated aromatic materials, T_1 values in excess of 1 min are common, meaning that the single-point method becomes excessively time consuming. Good quality CRAMPS results can still be produced with conventional nonquadrature detection, larger offsets and a low-Q probe, as illustrated by the spectra of perfluoronaphthalene and pentafluoroaniline. By using a specially-built probe and an MREV-8 sequence and sampling twice per cycle with an 8-pulse cycle time of 30 μs, it has been possible[50] to resolve inequivalent fluorines in the solid state. Spectra from perfluoronaphthalene are reproduced in Figure 11 and correspond to (a) MAS-only, with sample spinning at 5 kHz, (b–d) CRAMPS, with sample spinning at 1.7, 2.7, and 3.6 kHz, and (e) CRAMPS, with sample spinning at 3.6 kHz, but with a reduced offset to improve the centerband resolution. In the final case, resolution is sufficiently improved to allow the identification of four separate peaks due to the four inequivalent fluorines in the 1, 1′, 2, and 2′ positions (the molecule loses a symmetry axis in the solid state). The CRAMPS results obtained from a sample of pentafluoroaniline,[51] shown in Figure 12, allow the identification of separate centerband resonances due to fluorines ortho, meta, and

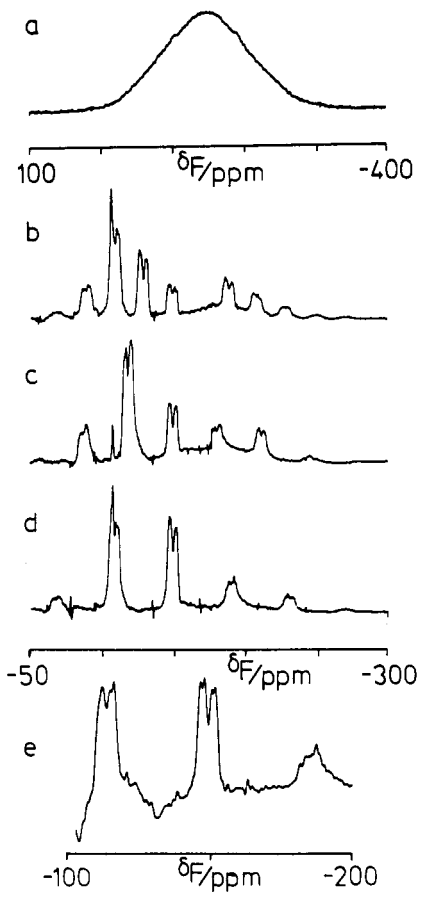

Figure 11. ^{19}F NMR (188.3 MHz) spectra of perfluoronaphthalene: (a) MAS spectrum with spinning at 5.0 kHz (no line narrowing is observed), (b–d) MREV-8 CRAMPS results obtained with spinning at 1.7, 2.7, and 3.6 kHz, respectively, (the peak at −107.7 ppm is due to a small amount of CaF_2 added as an internal reference), and (e) spectrum obtained with a smaller offset, giving better resolution under CRAMP conditions (reprinted from ref 50, copyright 1990 Academic Press).

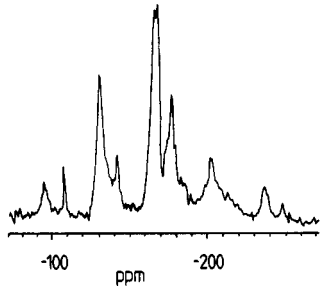

Figure 12. ^{19}F CRAMP (188.3 MHz) spectrum of pentafluoroaniline with spinning at 3.2 kHz. The peak at −107.7 ppm is due to a small amount of CaF_2 added as an internal reference. An MREV-8 sequence was used, with t_c = 30 μs.

para to the amino group. In both perfluoronaphthalene and pentafluoroaniline cases, resolution is degraded in the spinning sidebands, possibly due to spinner instability, spinning angle missetting or more complex interactions under multiple-pulse operation between spinning, offset, and shielding anisotropy. However, this does not prevent some analysis of the sideband intensities. For perfluoronaphthalene, the "average" shielding tensor was found to be axially symmetric, in good agreement with the earlier static multiple-pulse work,[10] due to rapid anisotropic molecular reorientation about the C_2 axis perpendicular to the planar molecule at room temperature.

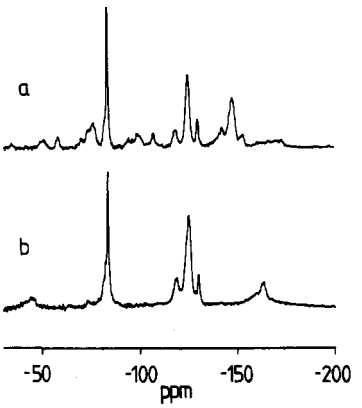

Figure 13. ^{19}F CRAMP (188.3 MHz) spectra of $C_8F_{17}SO_3Na$: (a) spinning at 2.1 kHz and (b) spinning at 4.0 kHz. In both cases an MREV-8 sequence was used, with t_c = 36 μs. Spectra were referenced by use of a small amount of CaF_2 added internally after recording the CaF_2-free spectra shown.

Fluorine-19 CRAMP NMR spectra have also been obtained[52] from the linear fluorocarbon solid $C_8F_{17}SO_3^-Na^+$. By spinning at rates up to 4.0 kHz, it has been possible to identify four resonances from CF_3CF_2–, –$(CF_2)_n$–, and –$CF_2SO_3^-$ moieties, using a conventional nonquadrature approach, with an MREV-8 cycle time of 36 μs. Use of MAS alone at the same spinning rate gave no narrowing of the static spectrum. Spectra are shown in Figure 13, with the spinning sidebands again broadened relative to the centerbands. Both the CF_3CF_2– resonances are significantly narrower than the other fluorine signals, possibly reflecting a greater degree of molecular mobility at the CF_3 end of the fluorocarbon chain.

A saturated fluorocarbon, of nominal composition $C_{14}F_{30}$, has also been studied[49,53] with use of a low-Q probe and nonquadrature detection. Some of the spectra obtained are included in Figure 14. In the melt at 200 °C, only five major resonances are observed. By using MAS at 4 kHz, broad baseline "rolls" begin to develop, indicating the onset of averaging the dipolar interactions at this moderate spinning rate. In addition, several sharp features are resolved, five of which correspond exactly to the melt state results, the remainder being identified as a known liquid contaminant. These sharp lines contribute less than 5% of the total signal intensity. CRAMPS results, obtained on different occasions, show that the solid-state structure of the material is more complex than of that in the melt, since up to seven separate major resonances are resolved, indicating some solid-state inequivalence. Figure 14d also illustrates the use of a small amount of calcium fluoride as an internal chemical shift standard (at −107.7 ppm relative to $CFCl_3$).

2. *Inorganic Fluorides*

Despite the use of MAS techniques in the study of inorganic systems, there appears to have been only one recent publication involving the application of CRAMPS experiments to the analysis of such problems.[54] This work demonstrated that CRAMPS has the capability to measure the relative amounts of calcium fluoride and fluoroapatite in mixtures in a quantitative fashion. Work was performed at 282.4 MHz using an unmodified CP/MAS probe with spinning around 5 kHz. A typical spectrum, acquired by using a multiply

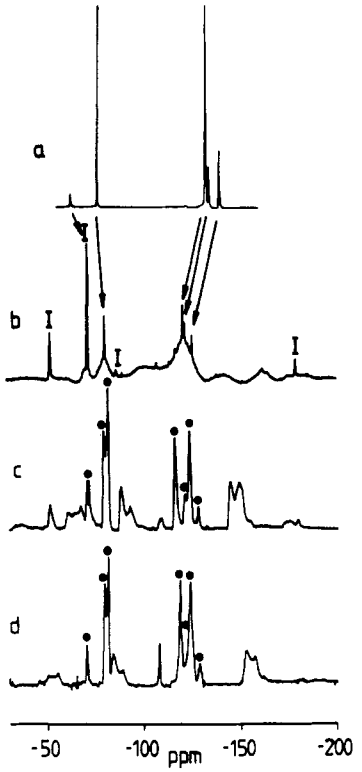

Figure 14. ^{19}F NMR (188.3 MHz) spectra of $C_{14}F_{30}$: (a) high-resolution spectrum obtained from the melt at 200 °C (note the scale change), (b) MAS spectrum with spinning at 4.0 kHz (several peaks due to a known contaminant are marked I), (c,d) spectra obtained on different occasions using CRAMPS, with spinning at 3.0 and 3.5 kHz. The peak at −107.7 ppm in d is due to a small amount of CaF_2 added as an internal reference. Centerbands are identified by ●.

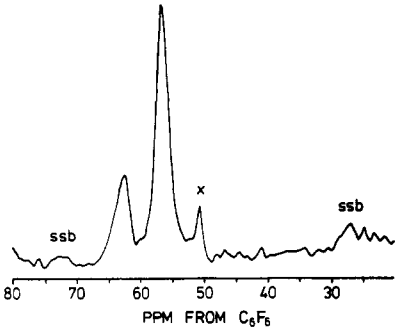

Figure 15. ^{19}F CRAMP (282.4 MHz) spectrum of a CaF_2/FAP mixture, with spinning at 4.9 kHz. Gaussian resolution enhancement has been applied. Spinning sidebands are marked ssb, and a rotor-frequency artefact is marked × (reprinted from ref 54, copyright 1990 Academic Press).

sampled MREV-8 sequence (cycle time = 48 μs) with post-processing to produce quadrature data, is shown in Figure 15. While the calcium fluoride resonance was found to exhibit the usual offset dependence, with the line width decreasing from over 1 kHz to less than 400 Hz as the carrier offset is reduced, the fluoroapatite signals did not change with offset. This is in agreement with the observation that relatively slow MAS will average dipolar interactions in fluoroapatite, meaning that the residual line width under CRAMPS is not likely to be homodipolar in origin, but is possibly due to broadening by adjacent protons, paramagnetic impurities, or dynamic effects. We add here, for interest, that the best resolution obtained by the present authors (at 188.31 MHz) from powdered calcium fluoride, added as an internal reference, is 87 Hz.

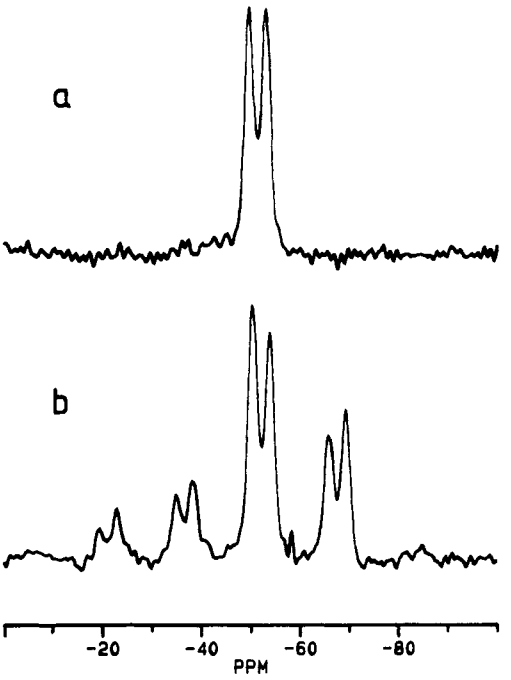

Figure 16. ^{19}F CRAMP (188.3 MHz) spectra of the polymeric material PPB. Single-point, quadrature detection was used (256 data points, 2 transients) with an MREV-8 cycle time of 36 μs. Section a shows spinning at 4.7 kHz, and section b shows spinning at 1.45 kHz. Spectra were referenced by use of a small amount of CaF_2 added internally after recording the CaF_2-free spectra shown.

3. Fluoropolymers

The first ever demonstration of the CRAMPS technique[13] involved observation of signals from the commonly used NMR polymer Kel-F. By using a home-built spectrometer and probe system, with an MREV-8 cycle time of 27 μs and spinning at 2.5 kHz, it was shown to be possible to resolve two resonances, separated by 23 ppm, with an intensity ratio of 2:1. The two peaks could be assigned to the CF_2 and $CFCl$ fluorines. Despite this early polymeric sample, there are still relatively few examples of the CRAMPS technique used in polymer science.

We have used the technique to look at the fluorine signals in a novel material, $-(C(CF_3)=C(CF_3))_n-$, designated PPB, obtained from the University of Durham. The static spectrum shows only a broad, featureless line, unaffected by slow spinning at rates up to 4 kHz. Early work[53] performed on this material using nonquadrature ^{19}F CRAMPS indicated that two centerband resonances were obtained, assigned to CF_3 groups in differing regions of the polymer. Sideband signals were broadened, not allowing the observation of further shielding tensor differences. Use of the single-point method with quadrature detection has led to an improvement in the quality of the spectra produced, now allowing clear differences to be seen between the sidebands associated with the different centerband signals and offering the ability to deduce shielding tensor information, thus helping to define the polymer structure. As seen from Figure 16, spinning at 4.7 kHz results in all the signal intensity being contained in the centerbands, giving a relative peak ratio of 1:1. With 1.45-kHz spinning, differences in the shielding envi-

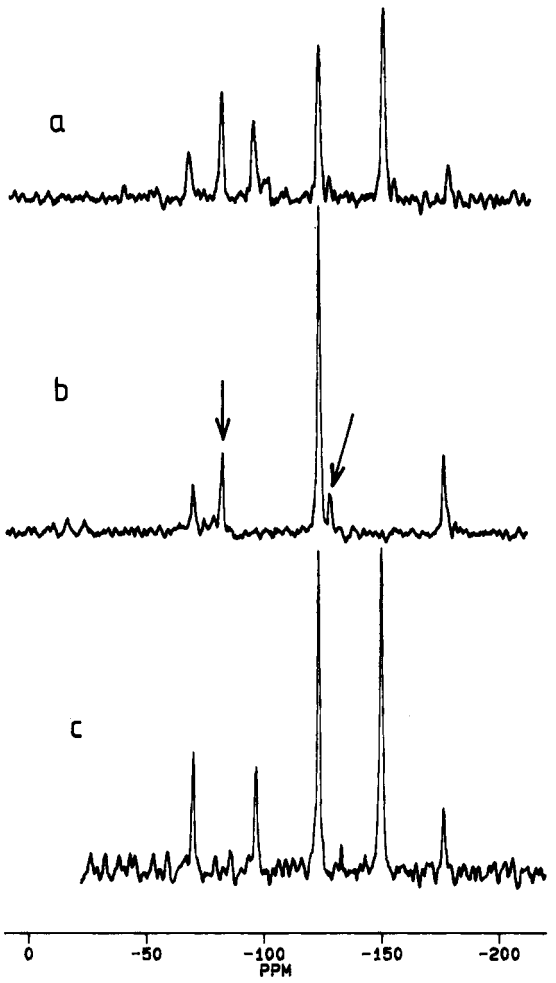

Figure 17. ^{19}F CRAMP (188.3 MHz) spectra of short- and long-chain PTFE: (a) $C_{20}F_{42}$ with spinning at 2.6 kHz, (b) $C_{20}F_{42}$ with spinning at 5.1 kHz, and (c) highly pure, highly crystalline long-chain PTFE with spinning at 2.5 kHz. In each case, single-point, quadrature detection was used (256 data points, 2 transients) with an MREV-8 cycle time of 36 μs. Spectra were referenced by using the $(CF_2)_n$ isotropic shift value (−123.2 ppm) obtained using MAS alone at 15.4 kHz. Chain-end signals are indicated by arrows in b.

ronments or molecular mobilities lead to different sideband patterns from each resonance.

Multiple-pulse methods have been successfully used[55-59] to probe morphology and orientation in static samples of polytetrafluoroethane (PTFE). The CRAMPS experiment offers the potential to perform similar studies with higher sensitivity and resolution. To illustrate the potential of CRAMPS in PTFE analysis, two samples have been studied with use of single-point quadrature detection; one a short-chain PTFE analogue, $C_{20}F_{42}$, and the other a highly crystalline, highly pure commercial PTFE powder. Spectra of $C_{20}F_{42}$ are shown in Figure 17 and correspond to samples spinning at (a) 2.6 and (b) 5.1 kHz. It is possible to identify separate resonances due to the CF_3CF_2– chain ends and the main-chain CF_2 fluorines, with line widths less than 300 Hz. Given the signal-to-noise and acquisition-time limitations, it is estimated that such end-group features would only be visible down to the 1–5% level with CRAMPS. Clearly, fast spinning would be superior in cases with lower levels, since signal averaging is more straightforward, although lines may not be narrowed as efficiently as in the CRAMPS case. In the slower spinning case, an extensive sideband pattern is observed from the main-chain CF_2 fluorines due to a large shielding anisotropy. The crystalline PTFE powder also gives spectra with narrow lines and spinning sidebands, as shown in Figure 17c, although any end-group effects are now lost, since the polymer has a molecular weight in excess of 500 000. The sideband intensities may be used to calculate shielding tensor components, enabling studies on PTFE morphology to be performed, as in the earlier nonspinning, multiple-pulse studies.

C. Future Developments

The CRAMPS results outlined in the above sections show that excellent resolution can be obtained from fluorinated samples, giving resolution better than that achieved by MAS alone where the same samples have been studied by both techniques, although, more generally, this is likely to depend on the degree of molecular mobility present. The calculation of shielding tensors by slow-spinning sideband analysis is expected to increase in popularity, reflecting the growing usage of this method[52] in more conventional MAS solid-state NMR. As illustrated with ^1H CRAMPS,[60] spinning samples at angles other than the magic angle leads to line-shape changes, also offering the ability to measure shielding tensor components. By combining CRAMPS experiments with rotor synchronization, it should be possible to extend PTFE (and other) spinning sideband analyses to investigate orientation effects in drawn samples. More work is clearly required to investigate fully the effects on CRAMPS spinning sidebands of changing morphology, for example in going from crystalline to amorphous PTFE.

One important problem still to be addressed is that of proton decoupling during ^{19}F CRAMPS acquisition. Unlike fast MAS studies, heteronuclear dipolar interactions are only partially removed by spinning combined with fluorine heteronuclear decoupling (depending on the magnitude of the proton–proton interactions). The rigid samples considered above were all perfluorinated, or had fluorine-containing moieties distant from protons. High-power proton decoupling has long been used in CP/MAS NMR, and has been used to decouple protons in a multiple-pulse ^{31}P study[43] (including CRAMPS). This is technically more difficult with fluorine observation and proton decoupling, due to the closeness of the resonant frequencies (188.3 and 200.1 MHz at 4.7 tesla), although a circuit has been developed[61] for simultaneous decoupling of both protons and fluorines while observing carbon-13 signals. A dual-channel facility would obviously extend the range of samples that could be studied to include the many systems that have both protons and fluorine in close proximity, opening up possibilities in pharmaceuticals, biochemistry, catalysis, polymer science, and solid-state chemistry.

IV. Summary

High-resolution ^{19}F solid-state NMR has clearly come of age, with both fast MAS and CRAMPS techniques capable of yielding resolution comparable with that routinely obtained in solid-state ^{13}C CP/MAS NMR. The advent of fast-spinning probes, specialized CRAMPS probes and stable, yet flexible and powerful

spectrometer rf systems has meant that these previously demanding techniques may now be more routinely implemented than in the past. Where the same samples have been studied by both techniques, ^{19}F CRAMPS has produce superior resolution, in line with previous work with ^{1}H CRAMPS on rigid materials,[42] reflecting the superior ability of multiple-pulse sequence to suppress strong homodipolar coupling. Due to the inherently lower signal-to-noise ratios obtained with the CRAMPS technique, and the difficulties associated with obtaining artefact-free spectra (e.g. rotor lines), it is unlikely that CRAMPS will have the same impact as fast MAS on polymer microstructure and sequencing studies, especially at low levels of copolymerization. Rather it is in the analysis of the solid-state structure of smaller molecules that the CRAMPS technique should be more successful, where resolution may be more important than sensitivity. The application of these complementary, rather than competitive, NMR techniques promises a bright future for the analysis of fluorine-containing solids.

V. Acknowledgments

We thank Drs. R. H. Carr and W. J. Brennan (ICI plc) for allowing us to use results obtained on their materials to illustrate some potential application areas. The help and enthusiasm of Dr. G. J. Nesbitt in the early stages of our adventures with ^{19}F CRAMPS are gratefully acknowledged.

Note Added in Proof. Since this review was written we have become aware of two recent relevant publications, which describe ^{19}F MAS studies of zeolite-related materials synthesized in fluoride media,[62] and a stable CRAMPS rotor–stator system involving dynamic-angle spinning[63] (example illustrated: ^{19}F in yttrium oxyfluoride).

VI. References

(1) Emsley, J. W.; Phillips, L. *Progress in Nuclear Magnetic Resonance Spectroscopy*; Emsley, J. W., Feeney, J., Sutcliffe, L. H., Eds.; Pergamon: Oxford, 1971; Vol. 7.
(2) Andrew, E. R.; Bradbury, A.; Eades, R. G. *Nature* **1958**, *182*, 1659.
(3) Lowe, I. J. *Phys. Rev. Lett.* **1959**, *2*, 285.
(4) Schaefer, J.; Stejskal, E. O. *J. Am. Chem. Soc.* **1976**, *98*, 1031.
(5) Brunner, E.; Fenzke, D.; Freude, D.; Pfeifer, H. *Chem. Phys. Lett.* **1990**, *169*, 591.
(6) Waugh, J. S.; Huber, L. M.; Haeberlen, U. *Phys. Rev. Lett.* **1968**, *20*, 180.
(7) Mansfield, P. *J. Phys. C* **1971**, *4*, 1444.
(8) Rhim, W.-K.; Elleman, D. D.; Vaughan, R. W. *J. Chem. Phys.* **1973**, *58*, 1772; **1973**, *59*, 3740.
(9) Burum, D. P.; Rhim, W.-K. *J. Chem. Phys.* **1979**, *71*, 444.
(10) Mehring, M.; Griffin, R. G.; Waugh, J. S. *J. Chem. Phys.* **1971**, *55*, 746.
(11) Mehring, M. *Principles of High Resolution NMR in Solids*, 2nd ed.; Springer-Verlag: New York, 1983.
(12) Ryan, L. M.; Taylor, R. E.; Paff, A. J.; Gerstein, B. C. *J. Chem. Phys.* **1980**, *72*, 508.
(13) Gerstein, B. C.; Pembleton, R. G.; Wilson, R. C.; Ryan, L. M. *J. Chem. Phys.* **1977**, *66*, 361.
(14) Maricq, M. M.; Waugh, J. S. *J. Chem. Phys.* **1979**, *70*, 3300.
(15) Pines, A.; Gibby, M. G.; Waugh, J. S. *J. Chem. Phys.* **1973**, *59*, 569.
(16) Demco, D. E.; Tegenfeld, J.; Waugh, J. S. *Phys. Rev. B* **1975**, *11*, 4133.
(17) Ganapathy, S.; Schramm, S.; Oldfield, E. *J. Chem. Phys.* **1982**, *77*, 4360.
(18) Mueller, K. T.; Sun, B. Q.; Chingas, G. C.; Zwanziger, J. W.; Terao, T.; Pines, A. *J. Magn. Reson.* **1990**, *86*, 470.
(19) Llor, A.; Virlet, J. *Chem. Phys. Lett.* **1988**, *152*, 248. Samoson, A.; Lippmaa, E.; Pines, A. *Mol. Phys.* **1988**, *65*, 1013.
(20) Andrew, E. R. *Int. Rev. Phys. Chem.* **1981**, *1*, 195.
(21) Andrew, E. R.; Farnell, L. F.; Firth, M.; Gledhill, T. D.; Roberts, I. *J. Magn. Reson.* **1969**, *1*, 27.
(22) Pembleton, R. G.; Ryan, L. M.; Gerstein, B. C. *Rev. Sci. Instrum.* **1977**, *48*, 1286.
(23) Wind, R. A.; Anthonio, F. E.; Duijvestijn, M. J.; Smidt, J.; Trommel, J.; deVette, G. M. *J. Magn. Reson.* **1983**, *52*, 424.
(24) Dec, S. F.; Wind, R. A.; Maciel, G. E.; Anthonio, F. E. *J. Magn. Reson.* **1986**, *70*, 355.
(25) Wind, R. A. *Proceedings of the Experimental NMR Spectroscopy Conference*, Asilomar, CA, 1989.
(26) Zumbulyadis, N.; Roberts, P. M.; Ferrar, W. T. *J. Magn. Reson.* **1987**, *72*, 388.
(27) Zumbulyadis, N. Private communication.
(28) Yesinowski, J. P.; Mobley, M. J. *J. Am. Chem. Soc.* **1983**, *105*, 6191.
(29) White, D. J.; Bowman, W. D.; Faller, R. V.; Mobley, M. J.; Wolfgang, R. A.; Yesinowski, J. P. *Acta Odontol. Scand.* **1989**, *46*, 375.
(30) Yesinowski, J. P.; Wolfgang, R. A.; Mobley, M. J. *Adsorption on and Surface Chemistry of Hydroxyapatite*, Misra, D. N., Ed.; Plenum: New York, 1983; p 157.
(31) Yesinowski, J. P.; Moran, L. Private communication.
(32) Raudsepp, M.; Turnock, A. C.; Hawthorne, F. C.; Sheriff, B. L.; Hartmann, J. S. *Am. Mineral.* **1987**, *17*, 580.
(33) Clark, J. H.; Goodman, E. M.; Smith, D. K.; Brown, S. J.; Miller, J. M. *J. Chem. Soc., Chem. Commun.* **1986**, 657.
(34) Duke, C. V. A.; Miller, J. M.; Clark, J. H.; Kybett, A. P. *Spectrochim. Acta* **1990**, *46A*, 1381.
(35) Duke, C. V. A.; Miller, J. M.; Clark, J. H.; Kybett, A. P. *J. Mol. Catal.* **1990**, *62*, 233.
(36) Asseid, F. M.; Duke, C. V. A.; Miller, J. M. *Can. J. Chem.* **1990**, *68*, 1420.
(37) Dec, S. F.; Wind, R. A.; Maciel, G. E. *Macromolecules* **1987**, *20*, 2754.
(38) Jackson, P.; Brennan, W. J. Unpublished results.
(39) Kreinbrink, A. T.; Sazavsky, C. D.; Pyrz, J. W.; Nelson, D. G. A.; Honkonen, R. S. *J. Magn. Reson.* **1990**, *88*, 267.
(40) Gaarenstroom, P. D.; Letts, L. B.; Harrison, A. M. *Proceedings of the 32nd Annual Polyurethanes Technical Conference*, 1989; p 163.
(41) Jackson, P.; Carr, R. H. *Magn. Reson. Chem.*, in press.
(42) Dec, S. F.; Bronniman, C. E.; Wind, R. A.; Maciel, G. E. *J. Magn. Reson.* **1989**, *82*, 454.
(43) Harris, R. K.; Jackson, P.; Wilkes, P. J.; Belton, P. S. *J. Magn. Reson.* **1987**, *73*, 178.
(44) Burum, D. P.; Linder, M.; Ernst, R. R. *J. Magn. Reson.* **1981**, *44*, 173.
(45) Jackson, P.; Harris, R. K. *Magn. Reson. Chem.* **1988**, *26*, 1003.
(46) Jackson, P. *J. Magn. Reson.* **1990**, *90*, 391.
(47) Rhim, W.-K.; Burum, D. P.; Vaughan, R. W. *Rev. Sci. Instrum.* **1976**, *47*, 720.
(48) Burum, D. P. *Concepts Magn. Reson.* **1990**, *2*, 213.
(49) Harris, R. K.; Jackson, P. *NATO Adv. Study Inst. Ser.* **1990**, *C322*, 355.
(50) Harris, R. K.; Jackson, P.; Nesbitt, G. J. *J. Magn. Reson.* **1989**, *85*, 294.
(51) Jackson, P.; Nesbitt, G. J.; Harris, R. K. Unpublished work.
(52) Harris, R. K.; Jackson, P.; Merwin, L. H.; Say, B. J.; Haegele, G. *J. Chem. Soc., Faraday Trans.* **1988**, *84*, 3649.
(53) Jackson, P. Ph.D. Thesis, University of Durham, 1987.
(54) Smith, K. A.; Burum, D. P. *J. Magn. Reson.* **1989**, *84*, 85.
(55) English, A. D.; Vega, A. J. *Macromolecules* **1979**, *12*, 353.
(56) Vega, A. J.; English, A. D. *Macromolecules* **1980**, *13*, 1635.
(57) Brandolini, A. J.; Rocco, K. J.; Dybowski, C. *Macromolecules* **1984**, *17*, 1455.
(58) Brandolini, A. J.; Apple, T. M.; Dybowski, C. *Polymer* **1982**, *23*, 39.
(59) Brandolini, A. J.; Dybowski, C. *J. Polym. Sci., Polym. Lett. Ed.* **1983**, *21*, 423.
(60) Taylor, R. E.; Pembleton, R. G.; Ryan, L. M.; Gerstein, B. C. *J. Chem. Phys.* **1979**, *71*, 4541.
(61) Kendrick, R. D.; Yannoni, C. S. *J. Magn. Reson.* **1987**, *75*, 506.
(62) Delmotte, L.; Soulard, M.; Guth, F.; Seive, A.; Lopez, A.; Guth, J. L. *Zeolites* **1990**, *10*, 778.
(63) Gerstein, B. C.; Pan, H.-J.; Pruski, M. *Rev. Sci. Instrum.* **1990**, *61*, 2699.